

## Enhanced Conductivity at the Interface of $\text{Li}_2\text{O}:\text{B}_2\text{O}_3$ Nanocomposites: Atomistic Models

Mazharul M. Islam,<sup>1</sup> Thomas Bredow,<sup>2</sup> Sylvio Indris,<sup>3</sup> and Paul Heitjans<sup>4</sup>

<sup>1</sup>*Applied Centre for Structural and Synchrotron Studies, University of South Australia, Mawson Lakes Campus, Mawson Lakes, Adelaide, South Australia 5095, Australia*

<sup>2</sup>*Institut für Physikalische und Theoretische Chemie, Universität Bonn, Wegelerstr. 12, 53115 Bonn, Germany*

<sup>3</sup>*Department of Chemistry, State University of New York at Stony Brook, 100 Nichols Rd., Stony Brook, New York 11794-3400, USA*

<sup>4</sup>*Institut für Physikalische Chemie und Elektrochemie, Leibniz-Universität Hannover, Callinstraße 3-3a, 30167 Hannover, Germany*

(Received 2 November 2006; published 2 October 2007)

A theoretical investigation at density-functional level of Li ion conduction at the interfaces in  $\text{Li}_2\text{O}:\text{B}_2\text{O}_3$  nanocomposites is presented. The structural disorder at the  $\text{Li}_2\text{O}(111):\text{B}_2\text{O}_3(001)$  interface leads to reduced defect formation energies for Li vacancies and Frenkel defects compared to  $\text{Li}_2\text{O}$  surfaces. The average activation energy for  $\text{Li}^+$  diffusion in the interface region is in the range of the values for  $\text{Li}_2\text{O}$ . It is therefore concluded that the enhanced Li conductivity of  $\text{Li}_2\text{O}:\text{B}_2\text{O}_3$  nanocomposites is mainly due to the increased defect concentration.

DOI: [10.1103/PhysRevLett.99.145502](https://doi.org/10.1103/PhysRevLett.99.145502)

PACS numbers: 61.72.-y, 61.82.Rx, 66.30.Pa, 71.15.Mb

In the last decade, ion diffusion in nanocrystalline ceramics has received considerable interest. Conductivity in ceramic oxides has been observed in single-phase systems as well as in composites of different components [1–7]. Nanocomposite materials often show enhanced conductivity compared to the single-phase ceramic oxides which is attractive with respect to possible applications in battery systems, fuel cells or sensors. In recent experiments, it has been observed that the conductivity in  $\text{Li}_2\text{O}:\text{B}_2\text{O}_3$  [1–3] and  $\text{Li}_2\text{O}:\text{Al}_2\text{O}_3$  nanocomposites [6] is higher than in nanocrystalline  $\text{Li}_2\text{O}$ , although  $\text{B}_2\text{O}_3$  and  $\text{Al}_2\text{O}_3$  are insulators. This surprising effect was attributed to the increased fraction of structurally disordered interfacial regions and the enhanced surface area of the nanosize particles [3]. In nanocrystalline  $\text{Li}_2\text{O}$ , there are interfaces between similar crystallites, whereas,  $\text{Li}_2\text{O}:\text{B}_2\text{O}_3$  nanocomposites contain three types of interfaces: between the ionic conductor grains, between the insulator grains and between the ionic conductor and the insulator grains.

Several classical models have been employed to describe the enhanced ionic conductivity in composite materials. The continuum percolation model was used to describe the dependence of the dc conductivity of  $\text{Li}_2\text{O}:\text{B}_2\text{O}_3$  nanocrystalline composites on the insulator concentration [1]. A brick-layer type percolation model treating both the micro- and the nanocrystalline composites on the same footing [4] is also able to reproduce the experimental results for the conductivity as a function of composition. In a recent investigation [5], a more sophisticated Voronoi approach was used. All these stochastic models do not explicitly take into account the structure of the nanoparticles and of their surfaces. The aim of the present study was to investigate the effect of the atomic structure in the interface region on the ion mobility. We have developed atomistic models of the  $\text{Li}_2\text{O}:\text{B}_2\text{O}_3$  nanocomposite based on periodic slabs. Investigations were performed to clarify whether the observed enhancement of Li conductivity in the  $\text{Li}_2\text{O}:\text{B}_2\text{O}_3$  interface is due to a

higher defect concentration (thermodynamically controlled) or to smaller activation barriers for local hopping processes (kinetically controlled). Models as proposed in the present study allow a direct simulation of the defect formation and mobility at atomic scale without any experimental input. They can give insight into the local bonding situation at the interface which is difficult to obtain from experiments.

We have modeled [8] the  $\text{Li}_2\text{O}:\text{B}_2\text{O}_3$  nanocomposite interface as a combination of the energetically favorable  $\text{Li}_2\text{O}(111)$  surface [14] and the most commensurate  $\text{B}_2\text{O}_3(001)$  surface. A  $4 \times 4$  supercell of the primitive  $\text{Li}_2\text{O}(111)$  surface unit cell with surface lattice parameters  $a = b = 12.9 \text{ \AA}$  was used as model for the  $\text{Li}_2\text{O}$  surface [15]. The  $\text{B}_2\text{O}_3(001)$  surface was modeled with a  $3 \times 3$  supercell ( $a = b = 13.1 \text{ \AA}$ ). Thus with the present combination of surface supercells, the lattice mismatch is only 1.3%. It is assumed that the nanoparticles can adjust their structure to minimize surface stress. Therefore the interlayer distance  $Z$  and the common surface lattice parameters  $a = b$  were optimized [16]. Our model is infinite in two dimensions but nonperiodic in the direction of the surface normal. The atoms in the uppermost and lowest layers are exposed to vacuum. We therefore divided the atomic layers into an interface region and an outer region. The interface region containing 75 atoms is marked with a box in Fig. 1(a). It consists of two Li layers and one O layer of the  $\text{Li}_2\text{O}$  surface and one B layer and two O layers of the  $\text{B}_2\text{O}_3$  surface. The Li layer close to the  $\text{B}_2\text{O}_3$  surface is denoted as first layer, the other as second layer. All atoms in the interface region are fully relaxed. The remaining atoms in the outermost layers are kept fixed at bulklike positions in order to simulate the inner part of the nanoparticles. The final optimized structure is shown in Fig. 1(b). To our knowledge, this is the first atomistic model for the interface region between ionic conductor and insulator grains [19]. Metal-oxide interfaces and insulator-insulator oxide interfaces have been studied be-

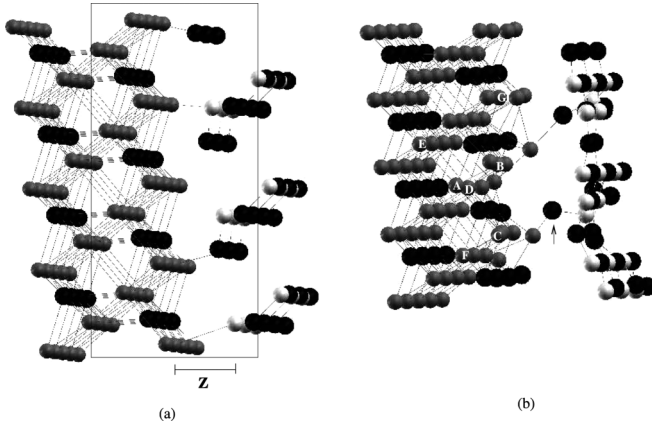


FIG. 1. The interface of  $\text{Li}_2\text{O}:\text{B}_2\text{O}_3$  nanocomposite; (a) after the optimization of  $Z$  and  $a$  and (b) after optimization of the interface region taking the optimized  $Z$  and  $a$ . Dark gray, black, and light gray spheres represent Li, O, and B, respectively.

fore with slab models at density-functional theory level and with classical force-fields [21,22].

As a main result of the optimization, we observe the formation of a new boron-oxygen bond in the interface region. One of the oxygen atoms of the  $\text{Li}_2\text{O}$  surface [marked by an arrow in Fig. 1(b)] is pulled out of the surface layer towards a neighboring boron atom of the  $\text{B}_2\text{O}_3$  surface. As consequence of this dislocation, the coordination of a Li atom in the second layer is reduced from four to three [Li (A) in Fig. 1(b)]. The remaining fourfold coordinated Li atoms in the second layer are denoted as type  $D$ ,  $E$ , and  $F$ . The threefold-coordinated lithium atoms of the first layer [ $B$ ,  $C$ , and  $G$  in Fig. 1(b)] do not change their coordination. It is assumed that reduced Li coordination and geometrical distortion due to the movement of the oxygen atom affect the energetics of defect formation in the interface region. This was investigated by calculating the lithium vacancy defect formation energy  $E_V$  [23] for types  $A$ – $G$ , and the Frenkel formation energy  $E_F$  [24] for representative Li atoms (types  $A$  and  $B$ ) in the interface region. In Table I, the calculated values of  $E_V$  and  $E_F$  of the  $\text{Li}_2\text{O}:\text{B}_2\text{O}_3$  nanocomposite are compared with theoretical values of bulk  $\text{Li}_2\text{O}$  [12,17] and the  $\text{Li}_2\text{O}(111)$  surface and also with available experimental data [18].  $E_V$  varies from 5.04 to 5.91 eV for the considered lithium types of the interface model. As expected, the defect formation energy for Li( $A$ ) with reduced coordination is the smallest (5.04 eV). Also, the other threefold-coordinated lithium atoms  $B$ ,  $C$ , and  $G$  in the top layer have smaller defect

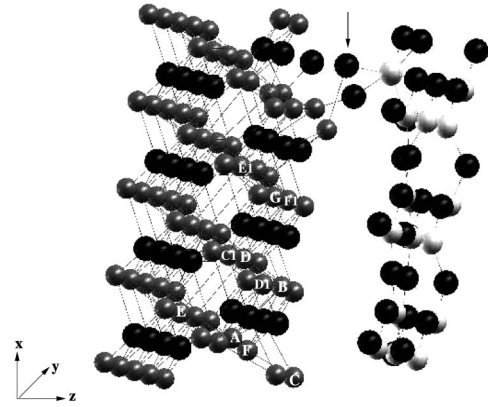


FIG. 2. Possible pathways for  $\text{Li}^+$  migration in the  $\text{Li}_2\text{O}:\text{B}_2\text{O}_3$  interface.

formation energies (5.08, 5.16, and 5.50 eV, respectively) than the fourfold coordinated lithium atoms  $D$ ,  $E$ , and  $F$  in the second layer (5.70, 5.63, and 5.91 eV, respectively). Li( $B$ ) and Li( $C$ ) are closer to the dislocated oxygen than Li( $G$ ) and, correspondingly, their bond strength is smaller.

For all considered sites  $E_V$  is smaller in the  $\text{Li}_2\text{O}:\text{B}_2\text{O}_3$  interface than in the  $\text{Li}_2\text{O}$  bulk (6.0 eV, Table I), and of the corresponding lithium atoms ( $A1$  and  $G1$ ) in the  $\text{Li}_2\text{O}(111)$  surface (5.63 and 5.16 eV, respectively). A similar effect was observed for the Frenkel defect formation (Table I).  $E_F$  is much smaller in the  $\text{Li}_2\text{O}:\text{B}_2\text{O}_3$  nanocomposite (1.17 eV) than in bulk  $\text{Li}_2\text{O}$  (2.24 eV). Our calculated bulk value is in agreement with experiment (2.53 eV) [18], and a previous DFT-LDA study (2.20 eV) [17]. As found for the vacancy formation,  $E_F$  in  $\text{Li}_2\text{O}:\text{B}_2\text{O}_3$  nanocomposite is smaller than in the  $\text{Li}_2\text{O}(111)$  surface (1.60 eV).

According to the defect formation energies, the interface region of  $\text{Li}_2\text{O}:\text{B}_2\text{O}_3$  nanocomposites contains higher concentrations of both defect types than bulk  $\text{Li}_2\text{O}$  and the  $\text{Li}_2\text{O}(111)$  surface. The similarity of the trends obtained for  $E_V$  and  $E_F$  is not surprising since both defects involve the formation of an empty Li lattice site [25]. In previous theoretical work [17] it has been shown that the migration barrier of the Li interstitial mechanism is higher than that of the vacancy mechanism. This is supported by more recent experimental investigations on the  $\text{Li}^+$  migration in  $\text{Li}_2\text{O}$  [3],  $\text{Li}_2\text{O}:\text{B}_2\text{O}_3$  [1,2] and  $\text{Li}_2\text{O}:\text{Al}_2\text{O}_3$  nanocomposites [6] where a vacancy mechanism was proposed. Therefore we concentrated on the vacancy mechanism in our model calculations. As first step, a single neutral Li atom was removed from the  $\text{Li}_2\text{O}:\text{B}_2\text{O}_3$  slab. This is a

TABLE I. Calculated formation energies of a Li vacancy,  $E_V$  (eV) and a Frenkel defect,  $E_F$  (eV)

	$\text{Li}_2\text{O}:\text{B}_2\text{O}_3^a$							$\text{Li}_2\text{O}$		$\text{Li}_2\text{O}(111)^a$		
	Li	$A$	$B$	$C$	$D$	$E$	$F$	$G$	Calc.	exp.	$A1$	$G1$
$E_V$		5.04	5.08	5.16	5.70	5.63	5.91	5.50	6.0 [12]		5.15	5.63
$E_F$		1.17							2.20 [17], 2.24 <sup>a</sup>	2.53 [18]	1.60	

<sup>a</sup>This work.

TABLE II. Comparison of measured and calculated activation energies  $\Delta E$  (eV) for Li hopping

		Li <sub>2</sub> O:B <sub>2</sub> O <sub>3</sub>					Li <sub>2</sub> O					Li <sub>2</sub> O:Al <sub>2</sub> O <sub>3</sub>			
		Calc.					Exp. [2]					Calc.	Exp. [3]	Exp. [6]	
<i>a</i>	<i>A</i> (second layer close to O4)	<i>G</i> (first layer far from O4)													
<i>b</i>	<i>B</i>	<i>C</i>	<i>D</i>	<i>E</i>	<i>F</i>	<i>B</i>	<i>C1</i>	<i>D1</i>	<i>E1</i>	<i>F1</i>					
$\Delta E_{ab}$	0.10	1.08	2.04	0.56	2.72	1.18	0.22	2.00	0.39	1.88	$0.34 \pm 0.04$	0.33 [12]	(0.34 [17])	0.31	$0.30 \pm 0.02$
$\Delta E_{ba}$	0.09	0.68	1.37	0.29	1.68	1.06	0.05	1.97	0.18	1.80					

simplification of the real situation where Li remains in the lattice and may affect the movement of other Li atoms. But in the present investigation, we are only interested in the activation barriers for hopping processes between regular lattice sites. Li migration may then occur from a tetrahedral site to a cation vacancy in the interface which is threefold-coordinated to oxygen atoms, or vice versa. Another possibility is a hopping process between an occupied and an unoccupied threefold-coordinated site of the first layer. In both cases, one or two oxygen atoms are shared by the migrating Li<sup>+</sup> and the cation vacancy [26].

In Fig. 2, selected lithium atoms are labeled to represent possible migration pathways for the Li<sup>+</sup> movement in the interface of Li<sub>2</sub>O:B<sub>2</sub>O<sub>3</sub> nanocomposite. As possible starting points, we selected two representative Li atoms, the second layer Li(*A*) which becomes threefold-coordinated due to the dislocation of one oxygen (O4), and the first-layer Li(*G*) which has a large distance (6.45 Å) from the dislocated oxygen. Migration of Li<sup>+</sup> can occur in a zigzag pathway, via hopping from site  $A \leftrightarrow B$ ,  $A \leftrightarrow C$ ,  $A \leftrightarrow E$ ,  $G \leftrightarrow B$ ,  $G \leftrightarrow C1$ , or  $G \leftrightarrow E1$ . Alternatively, migration can occur straight along the *x* direction ( $A \leftrightarrow D$  or  $G \leftrightarrow D1$ ), or along the *y* direction ( $A \leftrightarrow F$  or  $G \leftrightarrow F1$ ). The calculated values for the activation energy,  $\Delta E$ , for all these possible migration pathways are presented in Table II. Since the hopping processes can occur in both directions and the two Li sites are not equivalent in the Li<sub>2</sub>O:B<sub>2</sub>O<sub>3</sub> interface, we distinguished  $\Delta E_{ab}$  for the process ( $a \rightarrow b$ ) and  $\Delta E_{ba}$  for the migration in opposite direction [27]. Their smaller activation energies (0.1–1.2 eV) indicate that the zigzag pathways are more accessible than the migrations along the straight lines, either along the *x* direction ( $\Delta E = 1.4$ – $2.0$  eV) or the *y* direction ( $\Delta E = 1.7$ – $2.7$  eV). Several calculated  $\Delta E$ , e.g., for the processes  $B \rightarrow A$  (0.10 eV) and  $C1 \rightarrow G$  (0.22 eV), are much smaller than the experimental  $\Delta E$  of nanocrystalline Li<sub>2</sub>O, 0.31 eV [3]. They are also smaller than the measured activation enthalpies in Li<sub>2</sub>O:B<sub>2</sub>O<sub>3</sub> nanocomposites ( $0.34 \pm 0.04$  eV [2]) and in Li<sub>2</sub>O:Al<sub>2</sub>O<sub>3</sub> nanocomposites ( $0.30 \pm 0.02$  eV [6]). However, it has to be taken into account that in these experiments an average over the manifold of local hopping processes is obtained. Since the measurements have been performed at 300–500 K, it can be assumed that activation energies larger than 1 eV cannot be overcome in the time scale of NMR experiments. This excludes all straight pathways and also some of the zigzag pathways. The average of

the remaining nine calculated activation energies is 0.28 eV, in close agreement to the reported experimental values.

In summary, we have developed an atomistic model of nanocrystalline Li<sub>2</sub>O:B<sub>2</sub>O<sub>3</sub> composites. With this model, a quantum-chemical investigation of the defect properties and ionic conductivity in the interface region was performed. It was found that Li-O bonds are weakened and simultaneously B-O bonds are formed at the boundary between the two surfaces. This preference of oxygen bonding with B (or Al in Li<sub>2</sub>O:Al<sub>2</sub>O<sub>3</sub>) plays a key role in generating low-coordinated Li [28]. The removal of surface oxygen from Li<sub>2</sub>O is responsible for the increased vacancy defect concentration in Li<sub>2</sub>O:B<sub>2</sub>O<sub>3</sub> (or Li<sub>2</sub>O:Al<sub>2</sub>O<sub>3</sub>) nanocomposite materials. We propose that nanocomposites of ionic compounds (containing weakly bound and therefore mobile cations) with highly covalent compounds (with strong metal- or nonmetal-oxygen bonds) are in general promising candidates for high ionic conductivity. Our model calculations show that the most likely mechanism for Li<sup>+</sup> migration is in a zigzag pathway rather than in a straight line along a direction parallel to the interface plane. The averaged calculated activation energy for Li<sup>+</sup> migration in the Li<sub>2</sub>O:B<sub>2</sub>O<sub>3</sub> interface is similar to the experimental values of bulk Li<sub>2</sub>O, Li<sub>2</sub>O:B<sub>2</sub>O<sub>3</sub> and Li<sub>2</sub>O:Al<sub>2</sub>O<sub>3</sub> nanocomposites. We therefore conclude that the experimentally observed enhanced Li mobility in the Li<sub>2</sub>O:B<sub>2</sub>O<sub>3</sub> interface region is thermodynamically and not kinetically controlled.

M. M. I. thanks the State of Lower Saxony, Germany, for support from the Graduate Program of the Center for Solid-State Chemistry and New Materials, Leibniz University Hannover. The authors are grateful to Professor Andrea Gerson and Professor Roger Smart for fruitful discussion.

- [1] S. Indris, P. Heitjans, H. E. Roman, and A. Bunde, Phys. Rev. Lett. **84**, 2889 (2000).
- [2] S. Indris and P. Heitjans, J. Non-Cryst. Solids **307–310**, 555 (2002).
- [3] P. Heitjans and S. Indris, J. Phys. Condens. Matter **15**, R1257 (2003).
- [4] M. Ulrich, A. Bunde, S. Indris, and P. Heitjans, Phys. Chem. Chem. Phys. **6**, 3680 (2004).
- [5] S. Indris, P. Heitjans, M. Ulrich, and A. Bunde, Z. Phys. Chem. **219**, 89 (2005).

- [6] M. Wilkening, S. Indris, and P. Heitjans, *Phys. Chem. Chem. Phys.* **5**, 2225 (2003).
- [7] P. Knauth, *J. Electroceram.* **5**, 111 (2000).
- [8] For all calculations, the density-functional–Hartree-Fock one-parameter hybrid method PW1PW [9] was applied as implemented in the CRYSTAL package [10]; its accuracy for the description of solid-state properties has been demonstrated for  $B_2O_3$  [11],  $Li^+$  migration in  $Li_2O$  [12],  $Li_2B_4O_7$  [13].
- [9] T. Bredow and A.R. Gerson, *Phys. Rev. B* **61**, 5194 (2000).
- [10] V.R. Saunders *et al.*, *CRYSTAL 2003 User's Manual* (University of Torino, Torino, 2003); In CRYSTAL the Bloch functions are linear combinations of atomic orbitals. A combination of a 6-1G basis [31] for Li, an 8-411G basis for O [32] and a 6-21G basis for B [33] was used.
- [11] M.M. Islam, T. Bredow, and C. Minot, *Chem. Phys. Lett.* **418**, 565 (2006).
- [12] M.M. Islam, T. Bredow, and C. Minot, *J. Phys. Chem. B* **110**, 9413 (2006).
- [13] M.M. Islam, T. Bredow, and C. Minot, *J. Phys. Chem. B* **110**, 17518 (2006).
- [14] A. Lichanot, M. Gelize, C. Larrieu, and C. Pisani, *J. Phys. Chem. Solids* **52**, 1155 (1991).
- [15] The  $Li_2O$  slab model consists of six atomic layers and contains 32 f.u. In preliminary calculations, it was checked that the surface energy obtained with the six-layer model is converged. The  $Li_2O$  bulk lattice vector is 4.57 Å at PW1PW level, close to the experimental values, 4.573–4.619 Å [12]. The  $B_2O_3$  slab model has five atomic layers and contains 9 f.u. The surface lattice parameters  $a = b = 13.1$  Å correspond to the optimized bulk structure at PW1PW level,  $a_{\text{bulk}} = 4.35$  (exp. 4.34) Å,  $c_{\text{bulk}} = 8.39$  (8.34) Å [11].
- [16] The optimized values of  $Z$  and  $a = b$  are 5.0 and 12.4 Å corresponding to a substantial lateral contraction of 3%–4%. For comparison we calculated the defect formation energy of Li A (Table I) with lattice constant  $a = 13.0$  Å. Although the total energies of the defected and the stoichiometric reference model changed substantially, the calculated defect formation energy only slightly increased from 5.04 to 5.07 eV.
- [17] A. De Vita, M.J. Gillan, J.S. Lin, M.C. Payne, I. Stich, and L.J. Clarke, *Phys. Rev. Lett.* **68**, 3319 (1992).
- [18] A.V. Chadwick, K.W. Flack, J.H. Strange, and J. Harding, *Solid State Ionics* **28–30**, 185 (1988).
- [19] In our model we assumed that (a)  $Li_2O$  and  $B_2O_3$  nanoparticles have surfaces comparable to crystalline surfaces, and (b) stable contacts between the surfaces are more readily formed if their geometries are as similar as possible. The first assumption is justified by experimental studies of oxide nanoparticles demonstrating that even particles with only a few nm diameter have approximately bulklike atomic structure [3]. In recent scanning tunneling microscopy studies [20], it was shown that anatase nanoparticles have well-defined surface planes. As for the second assumption, there are, of course, many ways in which different surfaces of the two oxides can be combined. However, it is reasonable to assume that the selected building principle leads to a representative model of the nanocomposite system which is general enough to be applied in the present case and also for other combinations of oxides.
- [20] A. Feldhoff, C. Mendive, T. Bredow, and D. Bahnemann, *Chem. Phys. Chem.* **8**, 805 (2007).
- [21] C. R. A. Catlow, S. A. French, A. A. Sokol, M. Alfredsson, and S. T. Bromley, *Faraday Discuss.* **124**, 185 (2003).
- [22] D. C. Sayle, C. R. A. Catlow, J. H. Harding, M. J. F. Healy, S. A. Maicananu, S. C. Parker, B. Slater, and G. W. Watson, *J. Mater. Chem.* **10**, 1315 (2000).
- [23] The defect formation energy  $E_V$  is calculated with the following equation,
- $$E_V = E(Li_{2-x}O:B_2O_3) + E(Li, g) - E(Li_2O:B_2O_3),$$
- where  $E(Li_{2-x}O:B_2O_3)$  and  $E(Li_2O:B_2O_3)$  denote the total energy of the  $Li_2O:B_2O_3$  nanocomposite with and without vacancy, respectively, and  $E(Li, g)$  is the energy of the free Li atom.
- [24] The Frenkel formation energy  $E_F$  is the energy needed to move a  $Li^+$  ion from its regular lattice site to an interstitial site. The lowest converged value was obtained for a distance of 3.15 Å (Li A) and 4.77 Å (Li B) between the interstitial and the regular sites.
- [25] Because of the different references, the absolute values of  $E_F$  are much smaller than those of  $E_V$ . The two defect types can be regarded as extreme cases of real lattice defects, where the dislocated Li is close to the vacancy (Frenkel defect) or at infinite distance (hole vacancy).
- [26] Spin polarization plays an important role for the  $Li^+$  migration. It was observed that the unpaired electron, created due to the cation vacancy, is localized on the  $2p$  orbital of one of the surrounding oxygen atoms. The same situation was observed for the  $Li^+$  diffusion in crystalline  $Li_2O$  [12] and  $Li_2B_4O_7$  [13].
- [27] For each process the activation energies  $\Delta E_{ab}$ ,  $\Delta E_{ba}$  were approximated as energy difference of a transition structure where Li is halfway between the two sites, and the initial situation where Li is on site  $a$  and site  $b$  is empty, or vice versa. Effects from the zero point energy were neglected.
- [28] The effect can be predicted from the average Li-O and B-O (or Al-O) bond strengths of the bulk materials. Taking into account the atomic coordination numbers, 4 (Li) and 8 (O) in  $Li_2O$ , and 3 (B) and 2 (O) in  $B_2O_3$ -I, and the enthalpies of atomization, 1154 kJ/mol [29] and 3127 kJ/mol [30], formal bond energies of 144 kJ/mol (Li-O) and 521 kJ/mol (B-O) are obtained for  $Li_2O$  and  $B_2O_3$ , respectively. At this point it is important to note that theoretically obtained binding energies are accurate enough to be used for such an analysis if experimental data are unavailable. This has been repeatedly demonstrated, e.g., in our own studies of  $Li_2O$  and  $B_2O_3$  bulk properties [11,12].
- [29] *CRC Handbook of Chemistry and Physics* (CRC Press, Inc., Boca Raton, FL, 1991–1992), 72nd ed.
- [30] V. S. Yungman, *Thermal Constants of Substances* (Wiley, New York, 1999), Vol. 4.
- [31] M. Prencipe, A. Zupan, R. Dovesi, E. Aprà, and V.R. Saunders, *Phys. Rev. B* **51**, 3391 (1995).
- [32] R. Dovesi, C. Roetti, C. Freyria-Fava, and M. Prencipe, *Chem. Phys.* **156**, 11 (1991).
- [33] J. S. Binkley, J. A. Pople, and W. J. Hehre, *J. Am. Chem. Soc.* **102**, 939 (1980).